Pakistan Veterinary Journal

ISSN: 0253-8318 (PRINT), 2074-7764 (ONLINE)
DOI: 10.29261/pakvetj/2026.243

RESEARCH ARTICLE

Integrated Transcriptome and Microbiome Analyses Reveal Segment-Specific Host–Microbial Responses to DSS-Induced Enteritis in Chickens

Jinshan Ran[1#], Yanli Du[1#], Tiao Ning[1], Jing Li[1], Dalia Fouad[2], Muhammad Sarfaraz Iqbal[3], Ping Xiao[4*] and Wei Huang[1*]

[1]College of Agronomy and Life Sciences, Kunming University, Kunming 650214, China; [2]Department of Zoology, College of Science, King Saud University, PO Box 22452, Riyadh 11495, Saudi Arabia; [3]State Key Laboratory of Microbial Metabolism, School of Life Sciences and Biotechnology, Shanghai Jiao Tong University, 800 Dongchuan Road, Minhang District, Shanghai 200240, China; [4]College of Biological Science and Food Engineering, Southwest Forestry University, Kunming 650224, China. [#]These authors contributed equally to this work
[*]Corresponding author: huangwei_kmu@163.com (WH); ping.xiao@swfu.edu.cn (PX)

ARTICLE HISTORY (26-1094)

Received: September 05, 2026
Revised: October 16, 2026
Accepted: October 19, 2026
Published online: October 24, 2026

Key words:
Gut microbiota
Host–microbial interaction
Intestinal inflammation
Segment-specific response
Transcriptomics

ABSTRACT

Intestinal inflammation in chickens can manifest unequally along the gastrointestinal tract, yet how each region coordinates host–microbial alterations remain unclear. Using a dextran sulfate sodium (DSS)-induced enteritis model, we profiled the jejunum, ileum and cecum via integrated histology, plasma cytokine measurements, transcriptomics, 16S rRNA sequencing and correlation-based network analyses. DSS challenge elicited a systemic inflammatory phenotype, with markedly elevated IL-6, TNF-α, IFN-γ and IL-10, superimposed on anatomically divergent outcomes: the jejunum underwent pronounced structural remodeling and the most extensive transcriptional reprogramming; the ileum displayed a metabolically oriented expression shift accompanied by microbial expansion; and the cecum showed substantial taxonomic turnover and an epithelium- and lipid-metabolism-related transcriptomic signature despite limited morphometric change. PPAR-mediated lipid regulation emerged as a shared small-intestinal theme. Integrative analyses disclosed segment-specific microbe–gene couplings linking cecal taxa to epithelial barrier genes, ileal Enterococcus to metabolic regulators and jejunal Streptococcus to lipid transport, suggesting that local dysbiosis may steer host functional trajectories and influence the downstream effects of enteritis. These findings offer a spatial framework for gut inflammation and underscore intestinal location as a critical determinant of host–microbiota interplay in poultry.

To Cite This Article: Ran J, Du Y, Ning T, Li J, Fouad D, Iqbal MS, Xiao P, Huang W, 2026. Integrated transcriptome and microbiome analyses reveal segment-specific host–microbial responses to DSS-induced enteritis in chickens. Pak Vet J, 46(10): 2571-2581. http://dx.doi.org/10.29261/pakvetj/2026.243

INTRODUCTION

Intestinal health is closely associated with nutrient utilization, immune function and overall physiological status in poultry. As routine antibiotic use in poultry production continues to decline, intestinal disorders and the development of non-antibiotic strategies for maintaining gut health have received increasing attention (Graham *et al.*, 2023; Moore, 2024). Experimental enteritis models provide a controlled approach for examining intestinal injury and for evaluating nutritional or microbiota-targeted interventions. Dextran sulfate sodium (DSS) is a chemical agent commonly used to induce intestinal inflammation through disruption of the mucosal environment and epithelial barrier (Braga *et al.*, 2026). Although DSS models were initially developed primarily for experimental colitis in rodents, they have increasingly been applied in chickens to investigate intestinal injury, inflammatory responses and barrier dysfunction (Menconi *et al.*, 2015; Nii *et al.*, 2020; Nii *et al.*, 2021; Liu *et al.*, 2022).

The chicken intestinal tract is highly heterogeneous in both physiological function and microbial organization (Burrows *et al.*, 2025). The jejunum and ileum are major sites of nutrient absorption and exhibit segment-specific expression of transporters involved in the uptake of carbohydrates, peptides, amino acids, fatty acids and minerals (Sadr *et al.*, 2025). In contrast, the ceca harbor a complex microbial community and constitute a major site of microbial fermentation, particularly for the conversion of non-starch polysaccharides into volatile fatty acids (Ahmad *et al.*, 2026). Recent multi-omics studies have

further demonstrated regional differences in intestinal epithelial gene expression and microbial community composition in chickens (Li X et *al.,* 2025). These intrinsic differences suggest that individual intestinal segments may respond differently to the same inflammatory challenge. Accordingly, changes detected in one intestinal region may not necessarily represent the biological response occurring throughout the gastrointestinal tract.

Despite increasing interest in poultry intestinal inflammation, most studies have focused on individual intestinal regions or on a limited biological level, such as histological injury (Goo *et al.*, 2024), inflammatory markers (Froebel *et al.*, 2024), microbial composition (Du *et al.*, 2024), or host gene expression (Zhu *et al.*, 2025). Microbiome and transcriptome analyses have expanded the ability to characterize intestinal responses (Yu *et al.*, 2023), but the spatial relationship between microbial dysbiosis and host transcriptional responses remains insufficiently resolved across different intestinal segments (Tabish *et al.*, 2026). It remains unclear whether experimentally induced enteritis produces a common host–microbial response along the chicken intestinal tract or whether the jejunum, ileum and cecum develop distinct patterns of tissue injury, host transcriptional remodeling and microbial disturbance under the same inflammatory exposure.

Therefore, the present study used a DSS-induced enteritis model to examine the jejunum, ileum and cecum within the same experimental framework. Intestinal histology and plasma inflammatory factors were combined with transcriptome sequencing and 16S rRNA gene sequencing to characterize host and microbial responses in each intestinal segment. Differential bacterial taxa and host genes were further integrated with intestinal morphological and inflammatory variables to examine segment-specific host–microbial associations. The objective was to define the spatial heterogeneity of intestinal responses to DSS-induced enteritis and to determine whether different intestinal segments exhibit distinct patterns of host transcriptional and microbial alteration.

MATERIALS AND METHODS

Animals, experimental design and DSS-induced enteritis model: A total of 20 healthy Xishuangbanna Game chickens at 7 days of age were obtained from Xishuangbanna Game Chicken Conservation Farm. Before the experiment, all birds were acclimated for 3 days under standard husbandry conditions. Birds were housed in cages with free access to feed and water. The basal diet was formulated according to feeding standard and contained no antibiotics or anti-inflammatory additives. Temperature, humidity, lighting schedule and routine management were maintained according to standard poultry husbandry practice.

After acclimation, birds were randomly assigned to two groups: a control group and a dextran sulfate sodium (DSS) group. Each group contained 10 birds. Birds in the DSS group were gavaged a DSS solution (2mL, 2.5% weight/volume) at the same time each day for 14 days. Birds in the control group received equal volume of sterile saline under the same conditions. DSS solution was freshly prepared daily during the treatment period. The dose, route and duration of DSS administration were based on previously reported chicken enteritis protocols, in which DSS causes mucosal injury and an inflammatory response (Menconi *et al.*, 2015; Zou *et al.*, 2018; Liu *et al.*, 2022).

During the experiment, birds were monitored daily for general behavior, feed intake, fecal consistency and mortality. Body weight and feed intake were recorded at the indicated time points. Clinical signs related to enteritis, including fecal consistency, activity, perianal contamination and mortality, were evaluated according to scoring criteria.

All animal procedures were conducted in accordance with institutional guidelines for animal care and use. The experimental protocol was approved by the Animal Care and Use Committee of Kunming University, approval number Kmu 2026001.

Sample collection: At the end of DSS treatment, 6 birds per group were selected for sampling. Birds were fasted for 12 h before sampling, with free access to water. After anesthesia, birds were euthanized by cervical dislocation, and the abdominal cavity was opened immediately under aseptic conditions.

The intestinal tract was carefully removed and separated into the jejunum, ileum and cecum. The jejunum was defined as the segment between the distal end of the duodenal loop and Meckel's diverticulum. The ileum was defined as the segment between Meckel's diverticulum and the ileocecal junction. Mid-jejunal, mid-ileal and mid-cecal segments were collected for downstream analyses. For the cecum, samples were collected from the middle region of the cecal pouch, avoiding the cecal tonsil region unless otherwise specified. The three segments were chosen to cover both the absorptive and the fermentative regions of the chicken intestine, because the jejunum and ileum are the main sites of nutrient absorption while the ceca contain the most abundant and diverse bacterial community.

Intestinal contents from the jejunum, ileum and cecum were aseptically collected into sterile tubes for microbiota analysis. Samples were immediately frozen in liquid nitrogen and stored at -80°C. For histological analysis, approximately 2cm of each intestinal segment was fixed in 4% paraformaldehyde. For transcriptome sequencing and inflammatory factor detection, intestinal tissues or mucosal samples were collected after gentle rinsing with sterile phosphate-buffered saline. These samples were snap-frozen in liquid nitrogen and stored at −80°C until analysis.

Histological examination and morphometric analysis: Jejunal, ileal and cecal samples fixed in 4% paraformaldehyde were dehydrated through a graded ethanol series, cleared in xylene, embedded in paraffin and sectioned at a thickness of 4μm. The sections were stained with hematoxylin and eosin (H&E) and examined under a light microscope. Representative images were obtained from three randomly selected fields per sample.

Histological morphology was evaluated according to mucosal integrity and the structural characteristics of the

intestinal epithelium, villi, crypts and intestinal wall. For quantitative morphometric analysis, the number of crypts of Lieberkühn, villus height and intestinal wall thickness were measured in the jejunum, ileum and cecum. Measurements were performed on well-oriented intestinal structures within the selected microscopic fields and the mean value obtained for each sample was used for subsequent statistical analysis.

Measurement of inflammatory indicators: Wing vein blood samples were homogenized in cold phosphate-buffered saline or lysis buffer and centrifuged at 12000×g for 15min at 4°C. The supernatants were collected for analysis. The concentrations of IL-6, TNF-α, IL-10, IFN-γ were measured using commercial ELISA kits according to the manufacturer's instructions. Total protein concentration was determined using the BCA method. Cytokine levels were normalized to total protein content and expressed as pg/mL.

16S rRNA gene sequencing and microbiota analysis: Microbial DNA was extracted from jejunal, ileal and cecal contents using a DNA extraction kit according to the manufacturer's protocol. DNA concentration and purity were assessed using NanoDrop and DNA integrity was checked by agarose gel electrophoresis.

The V3-V4 region of the bacterial 16S rRNA gene was amplified using primers (341F: CCTAYGGGRBGCASCAG; 806R: GGACTACNNGGGTATCTAAT). PCR products were purified, quantified and pooled in equimolar amounts. Sequencing libraries were constructed and sequenced by Novogene Co., Ltd. (Beijing, China) on an Illumina platform using paired-end sequencing.

Raw paired-end reads were demultiplexed and quality-filtered. Primer sequences, low-quality reads and chimeric sequences were removed. High-quality reads were processed using DADA2 (Callahan *et al.*, 2016) to generate amplicon sequence variants. Taxonomic classification was performed against the SILVA database (https://www.arb-silva.de/), release 138 database.

Alpha diversity was evaluated using Observed features, Chao1, Shannon and Simpson indices. Beta diversity was calculated based on Bray-Curtis distances and visualized using principal coordinate analysis. Differences in microbial community structure were tested by permutational multivariate analysis of variance (PERMANOVA). Differential bacterial taxa among groups were identified using LEfSe, with significance defined as $P<0.05$.

RNA extraction, library construction, transcriptome sequencing and RNA-seq analysis: Jejunal, ileal and cecal tissues were used for transcriptome sequencing. Total RNA was extracted using an RNA extraction kit according to the manufacturer's instructions. RNA concentration and purity were measured using NanoDrop and RNA integrity was assessed using Agilent 2100 Bioanalyzer. Only high-quality RNA samples were used for library construction.

RNA-seq library preparation and sequencing were performed by Novogene Co., Ltd. (Beijing, China). Briefly, mRNA was enriched from total RNA using oligo(dT) beads and fragmented into short fragments. First-strand cDNA was synthesized using random hexamer primers, followed by second-strand cDNA synthesis. After end repair, A-tailing, adaptor ligation, size selection and PCR amplification, sequencing libraries were constructed. Qualified libraries were sequenced on an Illumina platform using paired-end 150 bp sequencing.

Raw reads were processed to remove adaptor sequences, reads containing poly-N and low-quality reads. Clean reads were used for subsequent analysis. Q20, Q30, GC content and sequence duplication level were calculated to evaluate sequencing quality.

Clean reads were aligned to the chicken reference genome (GRCg7b; RefSeq accession GCF_016699485.2) using HISAT2. Gene-level read counts were generated using feature Counts.

Differential expression analysis was performed using DESeq2 based on raw read counts. For each intestinal segment, the DSS group was compared with the control group. Differentially expressed genes were identified using the criteria of $|\log2(\text{fold change})| \geq 1$ and adjusted $P<0.05$. Principal component analysis and sample correlation analysis were performed using normalized expression data.

Gene Ontology (GO) and Kyoto Encyclopedia of Genes and Genomes (KEGG) enrichment analyses were performed for differentially expressed genes. Enriched terms and pathways with adjusted $P<0.05$ were considered significant. To compare segment-specific transcriptional responses, the number, direction, overlap and functional enrichment of differentially expressed genes were analyzed separately for the jejunum, ileum and cecum. Genes related to epithelial barrier function, inflammatory response, innate immunity, extracellular matrix remodeling and metabolic regulation were further extracted for downstream integrative analysis.

Integrative microbiome-transcriptome analysis: To explore the relationship between microbial dysbiosis and host transcriptional responses, combined microbiome-transcriptome analysis was performed separately for the jejunum, ileum and cecum. Differentially abundant bacterial taxa and differentially expressed genes were first identified within each intestinal segment.

Before correlation analysis, low-abundance microbial features were filtered. Only taxa detected in at least 20% of samples and with a mean relative abundance higher than 0.001 were retained. Because microbiome data are compositional, microbial abundance data were transformed using centered log-ratio transformation before correlation analysis.

Spearman correlation analysis was used to evaluate associations between differential bacterial taxa and differentially expressed genes. P values were adjusted using the Benjamini-Hochberg method. Significant microbe-gene associations were defined as $|r| \geq 0.6$ and FDR < 0.05.

Significant microbe-gene or microbe-gene module associations were visualized using heatmaps. In addition, global associations between microbial community, host transcriptomic profiles and anatomical indices, inflammatory factors were assessed using Mantel test to compare the coupling strength between multiple measurements across intestinal segments.

Statistical analysis: Statistical analyses were performed using SPSS 26.0 and R version 4.2.3. Data were first tested for normality and homogeneity of variance. Normally distributed data with equal variance were analyzed using Student's T-test or one-way analysis of variance. Non-normally distributed data were analyzed using the Mann-Whitney U test or Kruskal-Wallis test. Multiple comparisons were corrected using the Benjamini-Hochberg method.

RESULTS

DSS treatment induced inflammatory responses and segment-specific intestinal morphological alterations: The experimental procedure, sample collection and model validation are summarized in Fig. 1A. Compared with the control group, DSS treatment markedly increased the plasma concentrations of IL-10, IL-6, TNF-α and IFN-γ ($P<0.001$; Fig. 1B).

Histological examination showed different morphological responses to DSS among the three intestinal segments (Fig. 1C-F). In the cecum, DSS treatment did not significantly affect the number of crypts of Lieberkühn, villus height, or intestinal wall thickness (Fig. 1D). In the ileum, crypt number and villus height did not differ significantly between groups, whereas intestinal wall thickness was significantly lower in DSS-treated chickens than in controls (Fig. 1E). More evident morphological alterations were observed in the jejunum. DSS treatment significantly reduced the number of crypts of Lieberkühn and intestinal wall thickness, while villus height was significantly increased ($P<0.05$, Fig. 1F). These results showed that DSS-associated intestinal morphological alterations differed among the cecum, ileum and jejunum.

Transcriptomic responses to DSS differed among intestinal segments: Principal component analysis showed marked differences in transcriptional profiles among the cecum, ileum and jejunum (Fig. 2A). PC1 and PC2 explained 26.01 and 21.15% of the total variation, respectively. Within each intestinal segment, DSS-treated and control samples occupied different positions in the PCA space, although the extent of separation varied among segments.

The number of differentially expressed genes (DEGs) differed considerably among intestinal segments (Fig. 2B). In the ileum, 571 genes were upregulated and 205 were downregulated in the DSS group relative to the corresponding control group. The jejunum showed the largest number of DEGs, with 629 upregulated and 215 downregulated genes. In contrast, the cecum showed fewer transcriptional changes, with 145 upregulated and 76 downregulated genes.

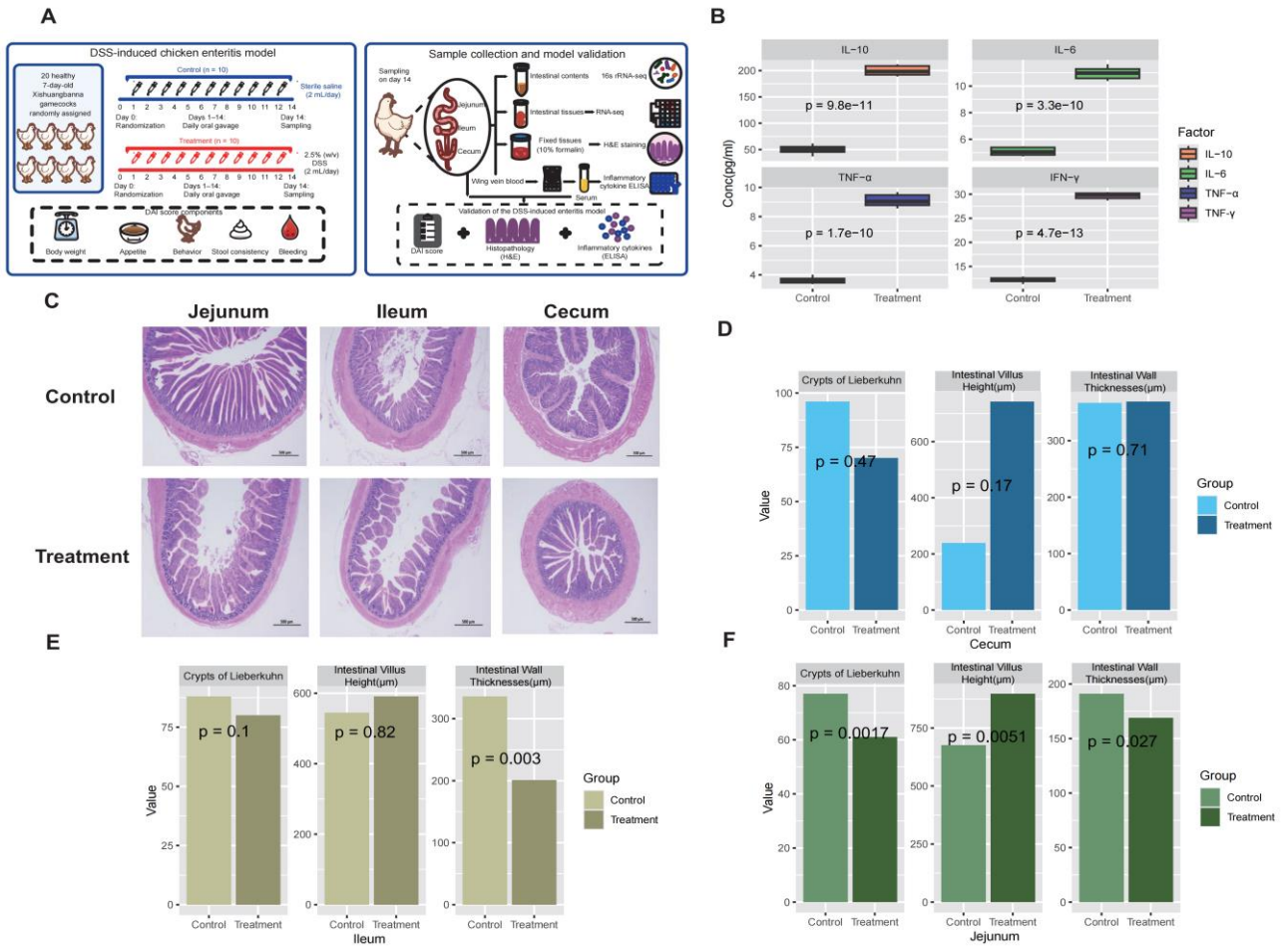


Fig. 1: Establishment and validation of the DSS-induced enteritis model in chickens. (A) Schematic illustration of the establishment, validation and subsequent analyses of the DSS-induced enteritis model. (B) Plasma concentrations of inflammation-related factors. (C) Representative hematoxylin and eosin (H&E)-stained sections of different intestinal segments. (D) Quantification of crypt number, intestinal wall thickness and villus height in the cecum. (E) Quantification of crypt number, intestinal wall thickness and villus height in the ileum. (F) Quantification of crypt number, intestinal wall thickness and villus height in the jejunum.

Microbial composition and alpha diversity showed segment-dependent responses to DSS: Genus-level microbial composition differed markedly among the cecum, ileum and jejunum (Fig. 3A). Cecal samples exhibited a more compositionally diverse microbial profile, whereas the ileal and jejunal communities contained larger proportions of several dominant genera. DSS treatment was also accompanied by changes in genus-level relative abundance profiles within individual intestinal segments.

Venn analysis showed limited overlap in genus-level taxa among the six groups, with only 19 taxa shared by all groups (Fig. 3B). The numbers of group-specific taxa were 807 and 564 in the DSS-treated and control cecal groups, respectively; 132 and 64 in the DSS-treated and control ileal groups, respectively; and 501 and 95 in the DSS-treated and control jejunal groups, respectively.

Chao1 richness differed primarily according to intestinal segment, with cecal samples showing higher values than ileal and jejunal samples (Fig. 3C). However, no significant DSS-associated difference in Chao1 richness was detected within the corresponding intestinal segments. In contrast, Shannon diversity showed significant treatment-associated changes in the small intestine (Fig. 3D). Shannon diversity was significantly higher in the DSS-treated ileum than in the corresponding control group ($P<0.01$) and was also significantly higher in the DSS-treated jejunum ($P<0.05$). No significant difference in Shannon diversity was observed between the DSS-treated and control cecal groups. These findings showed that the effect of DSS on alpha diversity differed among intestinal segments and was mainly reflected by increased Shannon diversity in the ileum and jejunum.

DSS-associated shifts in bacterial taxa differed among intestinal segments: Ordination analyses showed pronounced differences in microbial community structure among intestinal segments (Fig. 4A and B). In the PCA, PC1 accounted for 82.92% of the variation and separated the cecal communities from the ileal and jejunal communities, whereas PC2 explained 3.81% of the variation (Fig. 4A). The three-dimensional PCoA showed a similar distribution, with Axis 1, Axis 2 and Axis 3 explaining 94.90, 2.412 and 2.157% of the variation, respectively (Fig. 4B).

At the genus level, DSS-associated differential taxa varied among intestinal segments (Fig. 4C-E). In the cecum, the relative abundances of *Campylobacter*, *Anaerofilum, Colidextribacter* and Intestinimonas were significantly higher in DSS-treated chickens than in controls, whereas *Synergistes* was significantly lower ($P<0.05$, Fig. 4C). In the ileum, *Enterococcus* was significantly more abundant in the DSS group ($P<0.05$, Fig. 4D). In the jejunum, *Streptococcus* was significantly less abundant following DSS treatment ($P<0.05$, Fig. 4E).

LEfSe analysis further identified intestinal segment-specific microbial signatures associated with DSS treatment (Fig. 4F and G). In the cecum, *Clostridia*, *Oscillospiraceae*, *Campylobacter*, *Campylobacteraceae*, *Campylobacterales*, *Campylobacteria* and *Campylobacterota* were enriched in DSS-treated chickens, whereas *Atopobiaceae*, *Olsenella*, *Negativicutes*, *Selenomonadaceae*, *Megamonas* and *Veillonellales-Selenomonadales* were enriched in controls (Fig. 4F). In the ileum, *Ligilactobacillus, Enterococcus cecorum*, *Enterococcus*, *Enterococcaceae* and *Gammaproteobacteria* were enriched in the DSS group, whereas Firmicutes and Bacilli were enriched in the control group (Fig. 4G). Collectively, the differential-abundance analyses showed that DSS exposure was associated with distinct taxonomic changes in the cecum, ileum and jejunum.

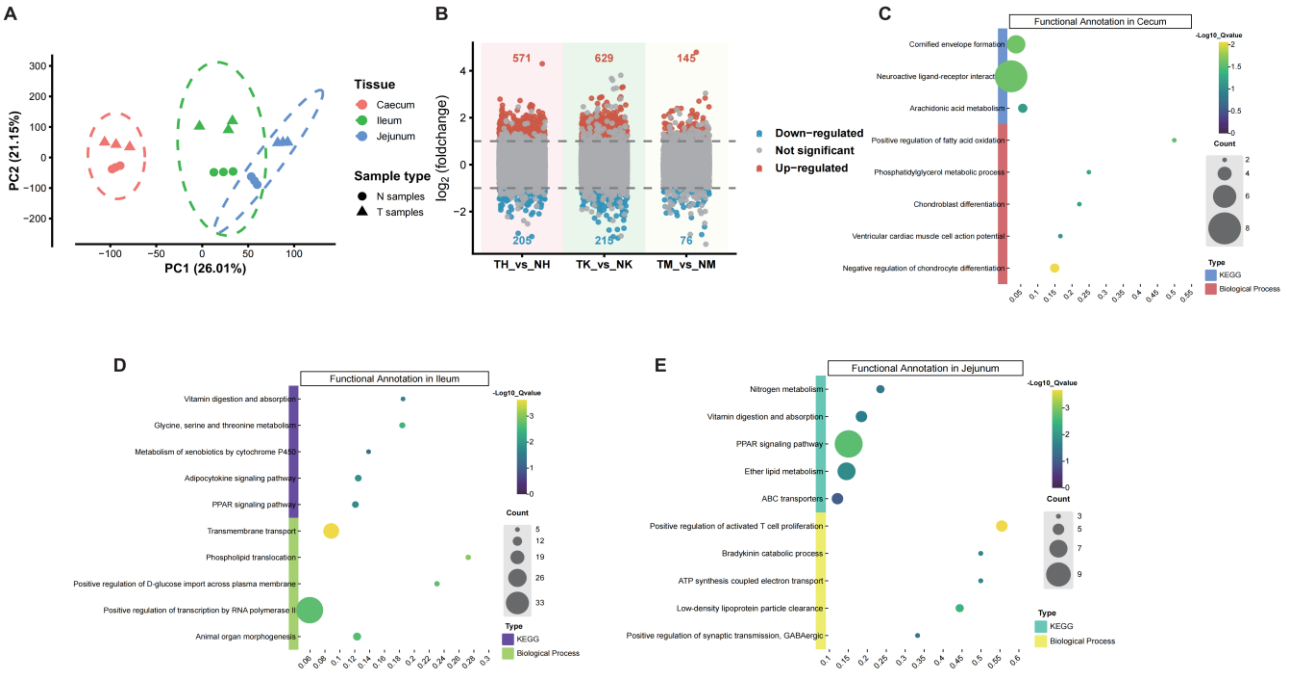


Fig. 2: Transcriptomic analysis of different intestinal segments in chickens with DSS-induced enteritis. (A) Principal component analysis (PCA) of transcriptomic profiles. (B) Scatter plots showing differentially expressed genes between the DSS-treated and control groups. (C) Functional enrichment analysis of differentially expressed genes in the cecum. (D) Functional enrichment analysis of differentially expressed genes in the ileum. (E) Functional enrichment analysis of differentially expressed genes in the jejunum. TM, DSS-treated cecum; TH, DSS-treated ileum; TK, DSS-treated jejunum; NM, control cecum; NH, control ileum; NK, control jejunum.

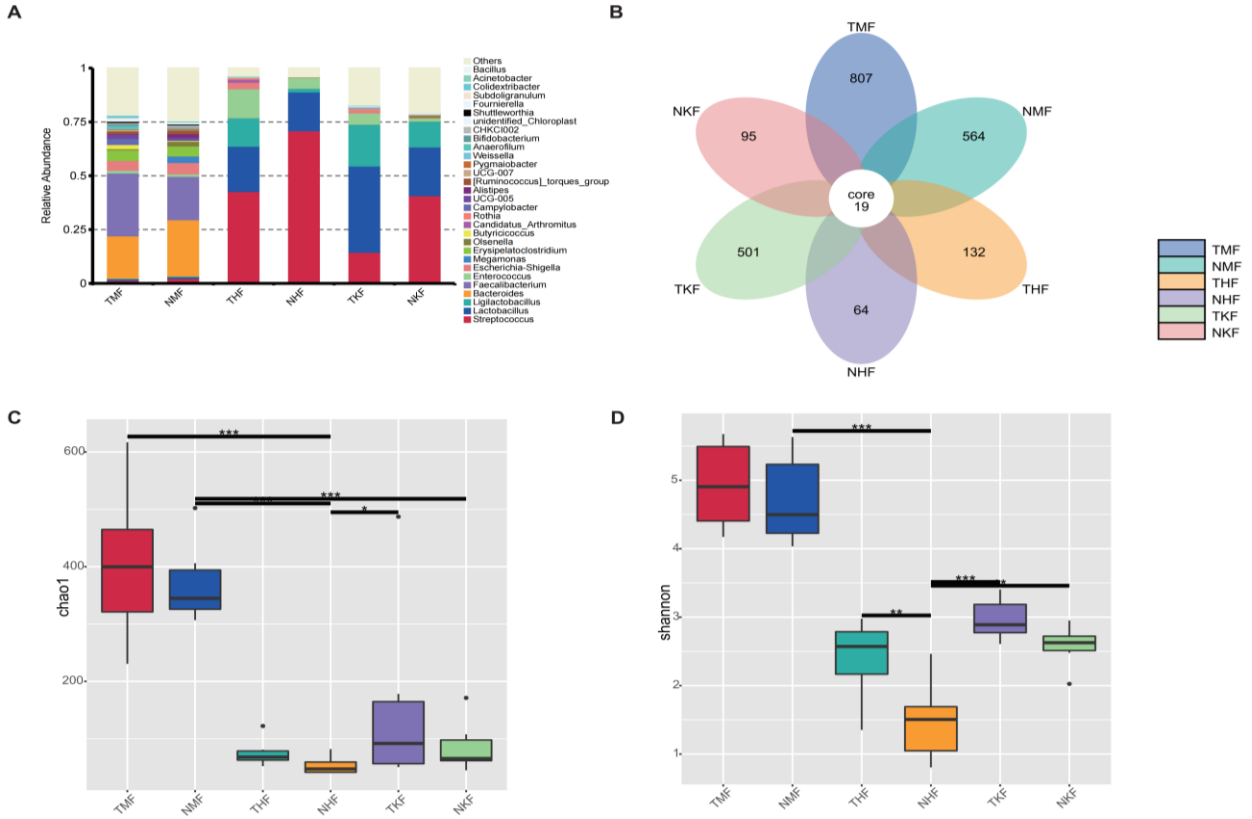


Fig. 3: Microbial composition and alpha diversity in different intestinal segments of chickens with DSS-induced enteritis. (A) Stacked bar plots showing the relative abundance of microbiota at the genus level. (B) Venn diagram showing shared and group-specific genus-level taxa among the six groups. (C) Alpha diversity assessed using the Chao1 index. (D) Alpha diversity assessed using the Shannon index. TMF, cecal contents from the DSS-treated group; THF, ileal contents from the DSS-treated group; TKF, jejunal contents from the DSS-treated group; NMF, cecal contents from the control group; NHF, ileal contents from the control group; NKF, jejunal contents from the control group.

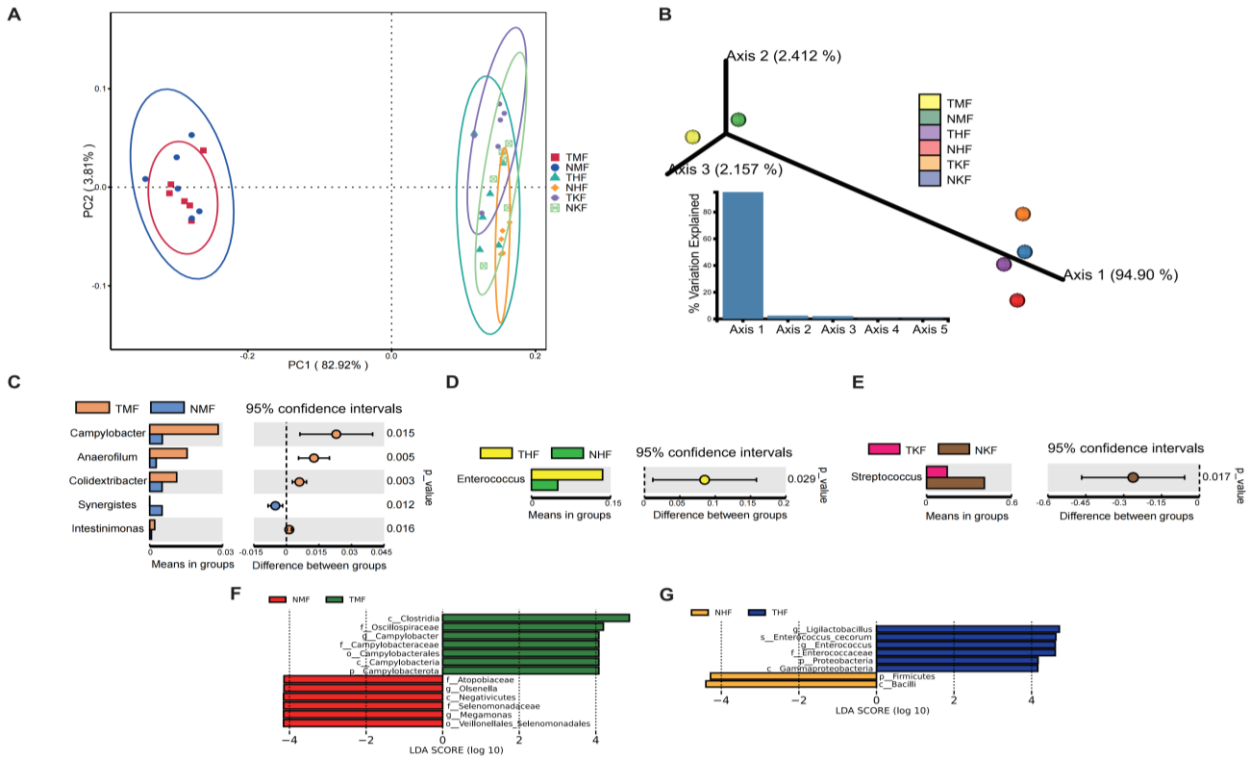


Fig. 4: Microbial community structure and differentially abundant taxa in different intestinal segments of chickens with DSS-induced enteritis. (A) Principal component analysis (PCA) of microbial communities. (B) Three-dimensional principal coordinate analysis (PCoA) of microbial communities. (C) Genus-level differential taxa between the DSS-treated and control groups in the cecum identified by t-test. (D) Genus-level differential taxa between the DSS-treated and control groups in the ileum identified by t-test. (E) Genus-level differential taxa between the DSS-treated and control groups in the jejunum identified by t-test. (F) LEfSe analysis of differentially abundant taxa in the cecum. (G) LEfSe analysis of differentially abundant taxa in the ileum. TMF, cecal contents from the DSS-treated group; THF, ileal contents from the DSS-treated group; TKF, jejunal contents from the DSS-treated group; NMF, cecal contents from the control group; NHF, ileal contents from the control group; NKF, jejunal contents from the control group.

Integrated analysis identified segment-specific associations among microbiota, host genes, intestinal morphology and inflammatory factors: Integrated correlation analysis revealed different association patterns among selected bacterial taxa, host genes, intestinal morphological parameters and inflammatory factors in the three intestinal segments (Fig. 5).

In the cecum, *Campylobacter* abundance was negatively correlated with KRT80 and KRT23 (P<0.001) and with CLDN2 (P<0.05; Fig. 5A). *Colidextribacter* was negatively correlated with KRT80 (P<0.01) and KRT23 (P<0.001). *Anaerofilum* was negatively correlated with KRT80 and KRT23 (P<0.05), whereas it was positively correlated with CLDN10 (P<0.01). In the ileum, *Enterococcus* showed positive correlations with CPT1A, PPARG, PPARA and PCK2 (P<0.01), but negative correlations with FABP6 (P<0.05) and ADIPOQ (P<0.01; Fig. 5B). Significant positive correlations were also observed among several of the selected host metabolic genes, including PPARG, PPARA and PCK2. A different association pattern was observed in the jejunum (Fig. 5C). *Streptococcus* was negatively correlated with CPT1A (P<0.01), MMP1 (P<0.05), PLIN2 (P<0.01), PPARG (P<0.01), CD36 (P<0.05), SLC27A4 (P<0.01) and PCK2 (P<0.01), whereas a positive correlation was observed between *Streptococcus* and FABP6 (P<0.05).

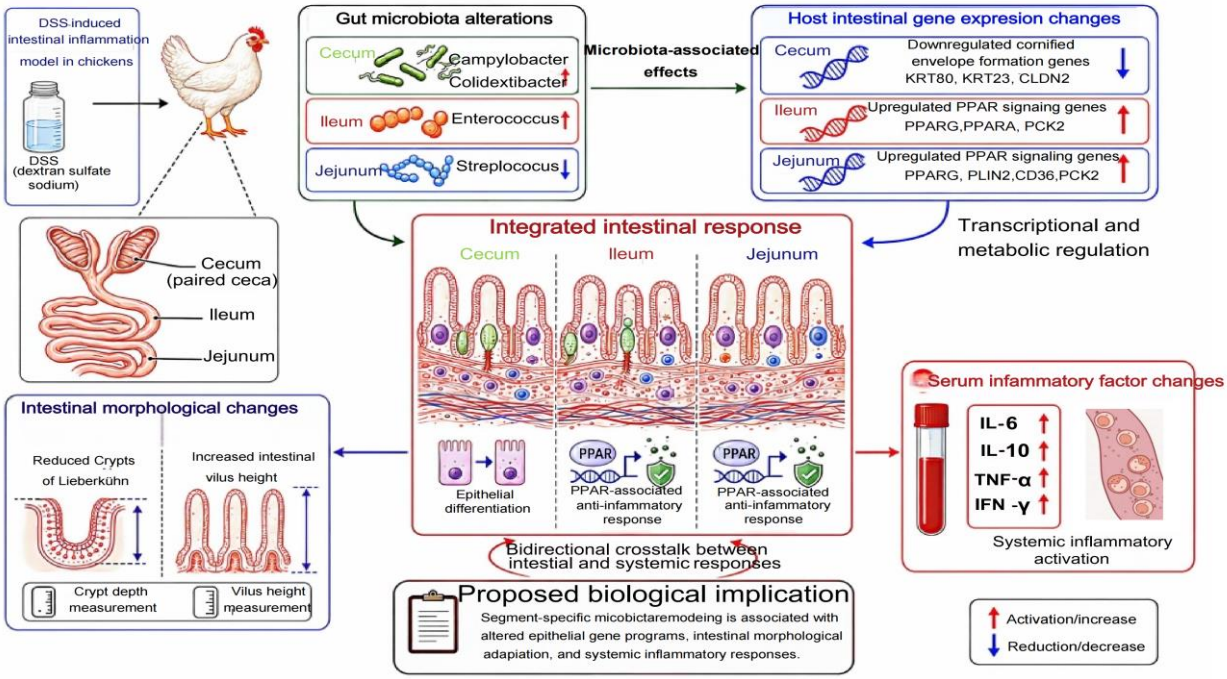


Fig. 6: Proposed interaction pathways among gut microbiota, host intestinal gene expression, intestinal morphology and plasma inflammatory factors in chickens with DSS-induced enteritis.

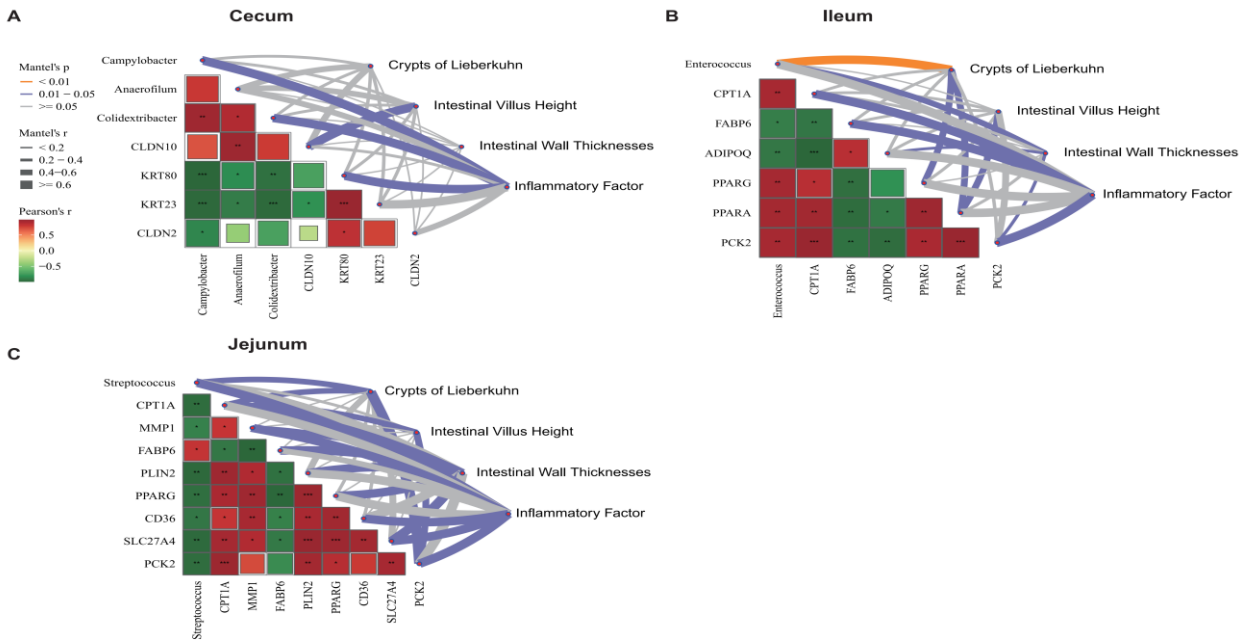


Fig. 5: Associations among key host genes, differential bacterial taxa, intestinal morphological parameters and inflammatory factors in different intestinal segments. Mantel test-based association analysis in the (A) cecum, (B) ileum and (C) jejunum.

Mantel tests further identified significant associations between selected microbial or host transcriptional variables and intestinal morphological or inflammatory parameters, with the pattern of significant relationships differing among the cecum, ileum and jejunum (Fig. 5A, B, C). In the ileum, *Enterococcus* was significantly associated with crypt number (Mantel's $P<0.01$). Additional significant associations (Mantel's $P<0.05$) involving intestinal morphology and inflammatory factors were observed in each intestinal segment. Overall, the integrated analyses demonstrated distinct segment-specific association patterns among microbial alterations, host gene expression, intestinal morphology and inflammatory status.

DISCUSSION

The present study provides a segment-resolved assessment of DSS-induced enteritis in chickens by integrating intestinal morphology, plasma inflammatory factors, host transcriptomic profiles and intestinal microbiota. A central finding was that the biological response to the same DSS exposure differed substantially among the jejunum, ileum and cecum. The jejunum exhibited the most evident morphological alterations and the largest transcriptional response, whereas the ileum showed a distinct combination of metabolic transcriptional responses and microbial changes. In contrast, the measured cecal morphological parameters remained relatively stable despite marked taxonomic shifts and a distinct host transcriptional profile. The associations among bacterial taxa, host genes, intestinal morphology and inflammatory factors also differed among intestinal segments. Collectively, these findings indicate that DSS-induced enteritis in chickens is characterized by segment-specific host and microbial responses rather than a uniform response throughout the intestinal tract.

Segment-Specific Intestinal Injury Following DSS Exposure: Recent studies using DSS-treated broilers have demonstrated that this chemical challenge can induce intestinal mucosal injury, altered villus and crypt morphology, increased intestinal permeability, impaired barrier-related characteristics and inflammatory responses (Chen *et al.*, 2023; Bai *et al.*, 2026; Li R *et al.*, 2026). In particular, Chen *et al.* (2023) reported alterations in villus height and crypt depth in both the jejunum and ileum, together with increased circulating IFN-γ and IL-6 following DSS exposure.

In the present study, however, the morphological response to DSS differed substantially among intestinal segments. The jejunum showed simultaneous changes in crypt number, villus height and intestinal wall thickness, whereas the ileal response was mainly characterized by reduced intestinal wall thickness. In contrast, none of the measured cecal morphological parameters differed significantly between DSS-treated and control chickens. The greater number of altered morphometric parameters in the jejunum is consistent with recent evidence that intestinal structure and functional characteristics are closely linked to regional physiological and gene-expression features in broilers (Akram *et al.*, 2024). Nevertheless, the present results do not imply that one intestinal segment is universally more susceptible to DSS than another; rather, they demonstrate that different structural components of the intestinal tract responded differently under the present experimental conditions.

Of particular interest, increased jejunal villus height occurred concurrently with reductions in crypt number and intestinal wall thickness. This combination does not conform to a simple pattern of uniform villus atrophy and therefore should not be interpreted using villus height alone as an indicator of intestinal condition, because intestinal histomorphology is generally evaluated using multiple complementary parameters, including villus height, crypt characteristics and their associated morphometric indices (Alagbe *et al.*, 2025). The intestinal epithelium is maintained through continuous cellular renewal and differentiation driven by intestinal stem cells and their progeny (Gehart and Clevers, 2019; Tao *et al.*, 2025). Recent work in DSS-treated broilers has further shown that mucosal structural injury can be accompanied by disruption of intestinal stem-cell homeostasis, including reductions in stem-cell abundance and impaired proliferation and differentiation (Li R *et al.*, 2026).

Plasma IL-6, TNF-α, IFN-γ and IL-10 were concurrently elevated after DSS treatment. Increased circulating IFN-γ and IL-6 have also been reported in DSS-challenged broilers (Chen *et al.*, 2023), while DSS exposure has been shown to increase serum TNF-α and IL-10 in chickens (Zou *et al.*, 2018). In the present study, the simultaneous elevation of pro-inflammatory factors and IL-10 indicates that both inflammatory and regulatory signals were represented in the plasma response, consistent with the established role of chicken IL-10 as an inducible feedback regulator of immune activation (Wu *et al.*, 2016). Because these factors were measured in plasma rather than separately within each intestinal segment, they provide evidence of an overall inflammatory phenotype but cannot identify the relative contribution of the jejunum, ileum or cecum.

Segment-Specific Host Transcriptional Responses: The transcriptomic results provided a second layer of evidence for spatial heterogeneity. The jejunum exhibited the largest number of DEGs, followed by the ileum, whereas substantially fewer DEGs were identified in the cecum. The biological significance of these responses, however, is more appropriately interpreted from their functional profiles than from DEG numbers alone.

Recent segment-resolved transcriptomic studies in chickens support the concept that intestinal regions can mount markedly different transcriptional responses to the same biological challenge (Overbey *et al.*, 2021; Jebessa *et al.*, 2024). For example, Jebessa *et al.* (2024) compared jejunal and cecal transcriptomes following *Eimeria maxima* infection and identified clear differences between the two intestinal regions in both the magnitude and functional composition of the transcriptional response. Although the inflammatory stimulus in that study differed from DSS, it provides independent evidence that anatomical location strongly influences the host intestinal transcriptional response in chickens.

In the present study, cecal DEGs were associated with cornified envelope-related functions, arachidonic

acid metabolism, fatty acid oxidation and phosphatidylglycerol metabolism. These findings indicate that epithelial-associated and lipid metabolic processes were represented in the cecal transcriptional response, but they do not establish whether individual pathways were protective or detrimental. The ileal response included PPAR signaling, adipocytokine signaling, xenobiotic metabolism and phospholipid and transmembrane transport-related functions. In the jejunum, PPAR signaling was accompanied by ether lipid metabolism, ABC transporters, nitrogen metabolism, activated T-cell proliferation and ATP synthesis-coupled electron transport.

The representation of PPAR signaling in both the ileum and jejunum suggests that lipid and metabolic regulation constituted a shared component of the small-intestinal response. PPAR-associated transcriptional responses have been linked to lipid transport, fatty-acid utilization and broader lipid metabolic regulation in broilers (Hu *et al.*, 2024; Su *et al.*, 2024). However, the other enriched pathways accompanying PPAR signaling differed between the ileum and jejunum in the present study. Thus, the data do not support a single common transcriptional program across the small intestine. Rather, related metabolic themes occurred within distinct segment-specific functional contexts, consistent with previous evidence that different intestinal regions in chickens can exhibit distinct molecular responses to the same biological challenge (Proszkowiec-Weglarz *et al.*, 2020; Jebessa *et al.*, 2024).

Intestinal Segment Determines the Pattern of Microbial Dysbiosis: The microbial results demonstrated a strong anatomical pattern. Cecal samples exhibited substantially greater richness and diversity than samples from the ileum and jejunum. A recent segment-resolved study of chickens likewise showed significantly greater alpha diversity in the cecum than in the small intestine and identified intestinal segment as a major determinant of microbial community structure (Luo *et al.*, 2025). More broadly, contemporary evidence indicates that chicken gut microbial composition is shaped by both host-associated and environmental factors, resulting in substantial ecological variation across intestinal environments (Ren *et al.*, 2026).

Against this anatomical background, the microbiota response to DSS was also segment dependent. Chao1 richness did not differ significantly between DSS-treated and corresponding control groups within the three intestinal segments, whereas Shannon diversity increased in the ileum and jejunum. Because these increases occurred together with changes in taxonomic composition, they should not be interpreted as simple restoration toward the control microbiota. Instead, the results indicate that DSS altered community organization in the two small-intestinal regions while having a different diversity response in the cecum.

The identities of the differential taxa reinforced this spatial pattern. In the cecum, DSS was associated with increased *Campylobacter*, *Anaerofilum*, *Colidextribacter* and *Intestinimonas* and reduced *Synergistes*, with LEfSe further identifying enrichment of multiple Campylobacter-related taxonomic groups. The ileal response was characterized most clearly by increased *Enterococcus*, whereas the jejunal response was characterized by reduced *Streptococcus*. Thus, no single differential genus characterized the DSS response across all three intestinal regions.

These genus-level changes should be interpreted conservatively. Amplicon sequencing based on the 16S rRNA gene provides valuable information on microbial community composition but has limited resolution for distinguishing closely related species or strains, while functional profiles inferred from 16S data are indirect and may not reliably capture actual microbial functional differences (Johnson *et al.*, 2019; Matchado *et al.*, 2024). Therefore, functional, pathogenic, or beneficial properties should not be assigned uniformly to the differential genera identified here. The central observation is instead that the taxonomic response to DSS differed among intestinal segments, consistent with the pronounced spatial heterogeneity of microbial communities along the chicken gastrointestinal tract (Wen *et al.*, 2021; Luo *et al.*, 2025; Ren *et al.*, 2026). Consequently, microbiome analysis restricted to a single intestinal region may capture only part of the microbial response associated with intestinal inflammation.

Segment-Specific Host–Microbial Associations: Integration of microbial and transcriptomic datasets showed that the bacterial taxa associated with host gene expression also differed among intestinal segments. These relationships represent statistical associations and should not be interpreted as evidence of direct microbial regulation of host transcription.

In the cecum, *Campylobacter*, *Colidextribacter* and *Anaerofilum* were associated with KRT and CLDN family genes. Claudin proteins are components of epithelial junctional complexes and altered claudin expression is commonly evaluated as part of intestinal barrier responses in broilers. For example, Zha *et al.* (2024) demonstrated that changes in jejunal claudin-3 and ZO-1 expression accompanied altered intestinal barrier status during immune challenge. In the present study, the correlations involving CLDN and KRT family members therefore link cecal taxonomic changes with epithelial-associated host responses. However, these associations do not establish whether the bacterial changes preceded the transcriptional response or resulted from an altered intestinal environment.

The ileum showed a different association structure. *Enterococcus* was positively correlated with CPT1A, PPARG, PPARA and PCK2 and negatively correlated with FABP6 and ADIPOQ. This pattern is particularly relevant because PPAR signaling and related metabolic functions were independently identified in the ileal transcriptomic enrichment analysis. The agreement between the pathway-level and correlation results therefore supports the presence of coordinated associations between ileal microbial changes and host metabolic responses, without establishing causal direction.

In the jejunum, *Streptococcus* was associated with several genes involved in lipid transport and metabolic regulation, including CPT1A, PPARG, CD36, SLC27A4 and PCK2. The composition and direction of these associations differed from those involving *Enterococcus*

in the ileum. Thus, even when related metabolic processes were represented in more than one intestinal segment, the microbial taxa associated with those host responses were not the same. This further supports the segment-specific nature of host–microbial relationships during DSS-induced enteritis.

Mantel analysis additionally identified associations between selected microbial or transcriptional variables and intestinal morphological or inflammatory parameters. The pattern of significant relationships differed among the cecum, ileum and jejunum, providing another level of correspondence among the biological datasets. Nevertheless, neither correlation analysis nor Mantel testing establishes causal direction. Microbial alterations could contribute to changes in the intestinal environment, host responses could reshape local microbial communities, or both processes could occur concurrently. Accordingly, the interaction pathways (Fig. 6) should be considered a working model integrating the observed relationships rather than a validated mechanistic pathway.

Biological Implications and Study Limitations: Taken together, the histological, transcriptomic, microbial and integrative analyses consistently demonstrate that intestinal location is an important determinant of the response observed during DSS-induced enteritis. The jejunum was characterized by prominent morphological and transcriptional alterations, the ileum by a distinct combination of metabolic transcriptional responses and microbial changes and the cecum by marked taxonomic shifts accompanied by epithelial- and metabolism-related transcriptional responses despite relatively limited changes in the measured morphological parameters. These findings indicate that examination of a single intestinal region may not fully represent the biological response occurring throughout the chicken intestinal tract.

Several limitations should be considered when interpreting these findings. First, major molecular and microbial analyses were conducted at the terminal stage of DSS exposure; therefore, the temporal order of microbial, transcriptional and morphological changes cannot be determined. Second, 16S rRNA gene sequencing provides limited taxonomic and functional resolution and microbial functional characteristics cannot be inferred directly from taxonomic abundance alone (Matchado *et al.*, 2024). Finally, the microbe-gene correlations and Mantel associations identify coordinated variation among biological variables but do not establish causality. Longitudinal sampling, higher-resolution microbial profiling and targeted experimental validation of selected host–microbial relationships would be required to resolve these questions.

Conclusions: This study demonstrates that DSS-induced enteritis in chickens is characterized by distinct segment-specific responses across the jejunum, ileum and cecum. The jejunum exhibited prominent morphological and transcriptional alterations, whereas the ileum showed a distinct combination of metabolic transcriptional responses and microbial changes. In contrast, the cecum displayed relatively limited changes in the measured morphological parameters but marked taxonomic shifts and a distinct host transcriptional profile. Integrated analyses further identified different associations among bacterial taxa, host genes, intestinal morphology and inflammatory factors in each intestinal segment. Collectively, these findings provide a segment-resolved view of chicken enteritis and indicate that intestinal location should be considered when evaluating host–microbial responses to intestinal inflammation. The associations identified here provide a basis for future targeted studies to determine the causal relationships underlying segment-specific intestinal responses.

Acknowledgement: This study was supported by the Yunnan Provincial Local Universities Joint Project (202501BA070001-074) and Talent Research Project of Kunming University (YJL2024022). The authors also extend their appreciation to “Ongoing Research Funding Program" (ORF-2026-965), King Saud University, Riyadh, Saudi Arabia.

Author Contributions: JR: Conceptualization, Investigation (animal feeding), Formal analysis, Methodology, Writing - original draft. YD: Investigation (feeding trial), Methodology, Validation. TN: Investigation (disease prevention and sampling), Methodology. JL: Formal analysis (including biostatistics). DF: Writing - original draft, Writing - review & editing. MSI: Writing - review & editing. PX: Formal analysis, Software, Visualization, Writing - review & editing. WH: Conceptualization, Data curation, Formal analysis, Project administration, Supervision, Writing – original draft, Writing – review & editing.

Competing interests: All authors declare no conflicts of interest to disclose.

Data and materials availability: Data are available from the authors upon reasonable request.

REFERENCES

Ahmad AA, Watson K, Khattak F, *et al.*, 2026. Integrative multi-omics analysis of dietary fiber induced modulations in the composition and function of chicken cecal microbiota. NPJ Biofilms and Microbiomes 12(1):73.

Akram MZ, Sureda EA, Corion M, *et al.*, 2024. Linking gastrointestinal tract structure, function, and gene expression signatures to growth variability in broilers: a novel interpretation for flock uniformity. Poultry Science 103(10):104158.

Alagbe EO, Sung JY, Lindsey K, *et al.*, 2025. Technical note: optimizing sample size for broiler chicken and pig intestinal histomorphometry and prediction equations. Journal of Animal Science 103:skaf160.

Bai X, Li R, Quan T, *et al.*, 2026. Butyrate improves dextran sulfate sodium-induced enterotoxicity in broilers. Molecular Immunology 195:209-220.

Braga GR, Farias MR, Fonseca L, *et al.*, 2026. Dietary tributyrin attenuates intestinal damage induced by dextran sulfate sodium and modulates growth performance in broilers. Poultry Science 105(11):107471.

Burrows P, Godoy-Santos F, Lawther K, *et al.*, 2025. Decoding the chicken gastrointestinal microbiome. BMC Microbiology 25(1):35.

Callahan BJ, McMurdie PJ, Rosen MJ, *et al.*, 2016. DADA2: High-resolution sample inference from Illumina amplicon data. Nature Methods 13(7):581-583.

Chen Y, Zha P, Xu H, *et al.*, 2023. An evaluation of the protective effects of chlorogenic acid on broiler chickens in a dextran sodium sulfate model: a preliminary investigation. Poultry Science 102(1):102257.

Du S, Song Z, Cen Y, *et al*., 2024. Susceptibility and cecal microbiota alteration to Eimeria-infection in Yellow-feathered broilers, Arbor Acres broilers and Lohmann pink layers. Poultry Science 103(7):103824.

Froebel LE, Calik A, Emami NK, *et al*., 2024. Evaluating performance, intestinal lesions, and immunity related genes in heritage and modern broiler breeds during a necrotic enteritis challenge. Poultry Science 103(12):104339.

Gehart H and Clevers H, 2019. Tales from the crypt: new insights into intestinal stem cells. Nature Reviews Gastroenterology & Hepatology 16(1):19-34.

Goo D, Ko H, Sharma MK, *et al*., 2024. Comparison of necrotic enteritis effects on growth performance and intestinal health in two different meat-type chicken strains Athens Canadian Random Bred and Cobb 500. Poultry Science 103(5):103599.

Graham D, Petrone-Garcia VM, Hernandez-Velasco X, *et al*., 2023. Assessing the effects of a mixed Eimeria spp. challenge on performance, intestinal integrity, and the gut microbiome of broiler chickens. Frontiers in Veterinary Science 10:1224647.

Hu W, Du L, Shao J, *et al*., 2024. Molecular and metabolic responses to immune stress in the jejunum of broiler chickens: transcriptomic and metabolomic analysis. Poultry Science 103(5):103621.

Jebessa E, Bello SF, Xu Y, *et al*., 2024. Comprehensive analysis of differentially expressed mRNA profiles in chicken jejunum and cecum following Eimeria maxima infection. Poultry Science 103(6):103716.

Johnson JS, Spakowicz DJ, Hong BY, *et al*., 2019. Evaluation of 16S rRNA gene sequencing for species and strain-level microbiome analysis. Nature Communications 10(1):5029.

Li R, Quan T, Chen Y, *et al*., 2026. Butyrate improves dextran sulfate sodium-induced imbalance of intestinal stem cell homeostasis in broilers. Poultry Science 105(2):106307.

Li X, Han X, Yan H, *et al*., 2025. From gut microbiota to host genes: A dual-regulatory pathway driving body weight variation in dagu chicken (*Gallus gallus* domesticus). Poultry Science 104(6):105067.

Liu L, Sui W, Yang Y, *et al*., 2022. Establishment of an enteric inflammation model in broiler chickens by oral administration with dextran sulfate sodium. Animals 12(24):3552.

Luo W, Sun S, Zhang L, *et al*., 2025. Intestinal segment-specific microbiota profiles correlate with body weight divergence in Ningdu yellow chickens. Poultry Science 104(12):106038.

Matchado MS, Rühlemann M, Reitmeier S, *et al*., 2024. On the limits of 16S rRNA gene-based metagenome prediction and functional profiling. Microbial Genomics 10(2):001203.

Menconi A, Hernandez-Velasco X, Vicuña E, *et al*., 2015. Histopathological and morphometric changes induced by a dextran sodium sulfate (DSS) model in broilers. Poultry Science 94(5):906-911.

Moore RJ, 2024. Necrotic enteritis and antibiotic-free production of broiler chickens: Challenges in testing and using alternative products. Animal Nutrition 16:288-298.

Nii T, Bungo T, Isobe N, *et al*., 2020. Intestinal inflammation induced by dextran sodium sulphate causes liver inflammation and lipid metabolism disfunction in laying hens. Poultry Science 99(3):1663-1677.

Nii T, Bungo T, Isobe N, *et al*., 2021. Slight disruption in intestinal environment by dextran sodium sulfate reduces egg yolk size through disfunction of ovarian follicle growth. Frontiers in Physiology 11:607369.

Overbey EG, Ng TT, Catini P, *et al*., 2021. Transcriptomes of an array of chicken ovary, intestinal, and immune cells and tissues. Frontiers in Genetics 12:664424.

Proszkowiec-Weglarz M, Schreier LL, Kahl S, *et al*., 2020. Effect of delayed feeding post-hatch on expression of tight junction– and gut barrier–related genes in the small intestine of broiler chickens during neonatal development. Poultry Science 99(10):4714-4729.

Ren J, He Q, Shang H, *et al*., 2026. Host genetic and environmental determinants of chicken gut microbiota: A review. Poultry Science 105(3):106432.

Sadr VS, Quinteros JA, Liu SY, *et al*., 2025. Nutrient transporters in broiler chickens: intestinal gene expression profiles, functional roles, and influencing factors. Journal of Animal Science and Biotechnology 16(1):165.

Su Y, Huang P, Wu Z, *et al*., 2024. Effect of dietary supplementation with sanguinarine on meat quality and lipid metabolism of broilers. Poultry Science 103(8):103925.

Tabish R, Lin Y, Rochell S, *et al*., 2026. Jejunal histopathology, metagenome, and mucosal transcriptome of broilers after an enteric challenge and fed diets with different types and concentrations. Poultry Science 105(9):107215.

Tao X, Hu G, Wang Z, *et al*., 2025. Effect of monochromatic light on self-renewal and differentiation of intestinal stem cells in broilers. Poultry Science 104(10):105499.

Wen C, Yan W, Mai C, *et al*., 2021. Joint contributions of the gut microbiota and host genetics to feed efficiency in chickens. Microbiome 9(1):126.

Wu Z, Hu T, Rothwell L, *et al*., 2016. Analysis of the function of IL-10 in chickens using specific neutralizing antibodies and a sensitive capture ELISA. Developmental & Comparative Immunology 63:206-212.

Yu H, Wang Q, Tang J, *et al*., 2023. Comprehensive analysis of gut microbiome and host transcriptome in chickens after Eimeria tenella infection. Frontiers in Cellular and Infection Microbiology 13:1191939.

Zha P, Liu W, Zhou Y and Chen Y, 2024. Protective effects of chlorogenic acid on the intestinal barrier of broiler chickens: an immunological stress model study. Poultry Science 103(8):103949.

Zhu R, Jing Y, Tang J, *et al*., 2025. Effects of *Akkermansia muciniphila* on growth, antioxidant status and jejunal transcriptome in LPS-stressed yellow-feathered broilers. Poultry Science 104(12):105954.

Zou X, Ji J, Wang J, *et al*., 2018. Dextran sulphate sodium (DSS) causes intestinal histopathology and inflammatory changes consistent with increased gut leakiness in chickens. British Poultry Science 59(2):166-172.